Journal of Materials Chemistry C

MoO_2 as a thermally stable oxide electrode for dynamic random-access memory capacitors

Journal:	*Journal of Materials Chemistry C*
Manuscript ID	TC-ART-08-2018-004167.R2
Article Type:	Paper
Date Submitted by the Author:	14-Nov-2018

Complete List of Authors:	Lee, Woongkyu; Northwestern university Cho, Cheol Jin; Korea Institute of Science and Technology Lee, Woo Chul; Korea Institute of Science and Technology, Center for Electronic Materials Hwang, Cheol Seong; Seoul National University, Department of Materials Science and Engineering Chang, Robert; Northwestern University, Materials Research Institute Kim, Seong Keun; Korea Institute of Science and Technology, Center for Electronic Materials

Journal Name

ARTICLE

MoO_2 as a thermally stable oxide electrode for dynamic random-access memory capacitors

Received 00th January 20xx,
Accepted 00th January 20xx

DOI: 10.1039/x0xx00000x

www.rsc.org/

Woongkyu Lee,†[a] Cheol Jin Cho,†[bc] Woo Chul Lee,[bc] Cheol Seong Hwang,[c] Robert P. H. Chang,[a] Seong Keun Kim*[b]

Metallic MoO_2 is proposed as a new oxide electrode for dynamic random-access memory (DRAM) capacitors. Although noble metal oxide electrodes including RuO_2 and $SrRuO_3$ have attracted interest as capacitor electrodes, these materials have critical instability problems of ease-reduction during the subsequent annealing process. In contrast, MoO_2 shows excellent thermal stability of the structural and chemical properties even after annealing at 400 °C in both forming gas and O_2 atmospheres. In addition, MoO_2 electrodes induce the formation of a high temperature phase with a high dielectric constant, rutile TiO_2, by atomic layer deposition at the relatively low temperature of 250 °C because of the structural homogeneity between MoO_2 and rutile TiO_2. These results demonstrate that the MoO_2 could be a promising electrode material for DRAM capacitors.

Introduction

Dynamic random-access memory (DRAM), composed of a capacitor and a transistor, has long served as the main memory type in modern computers. Scaling down of DRAM cells has been pursued to realize a desired increase in the memory density. A critical way to continue this scaling-down is to introduce novel materials that enable high performance.[1] At present, DRAM capacitors are composed of $ZrO_2/Al_2O_3/ZrO_2$ nanolaminate and TiN as the dielectric and electrode, respectively. The $ZrO_2/Al_2O_3/ZrO_2$ nanolaminate has a dielectric constant (k) of <40, which is not sufficient for further scaling. Therefore, higher-k materials such as rutile TiO_2 and $SrTiO_3$ have been studied as alternate dielectrics.[2-6] TiN has a low work function of 4.2 – 4.5 eV,[7] which is not high enough to suppress the leakage currents of the capacitors. In addition, an interfacial layer between the dielectric and TiN is easily formed during the growth of the dielectric layer on TiN. This interfacial layer could result in the deterioration of the dielectric performance, including a decrease in the effective k value and an increase in the leakage currents. Accordingly, the development of new electrode materials for the further scaling of DRAM cells is required.

Conducting oxides such as RuO_2 and $SrRuO_3$ have been considered as replacements for the capacitor electrode.[8-10] RuO_2 and $SrRuO_3$ have the same promising crystal structure as the dielectric materials rutile TiO_2 and $SrTiO_3$, respectively. The structural homogeneity leads to the in-situ crystallization of the high-k layers on the oxide electrodes even at relatively low temperatures, although these high-k layers are not generally crystallized by the conventional growth processes.[2, 11] The k value of the dielectric layers increases on the oxide electrodes due to the improvement in the crystallinity. In addition, unlike TiN, RuO_2 and $SrRuO_3$ have high work functions, which is advantageous in suppressing the leakage currents.

Despite these advantages of the oxide electrodes, a critical instability issue remains which must be addressed for the oxide electrodes to be implemented in DRAM capacitors. DRAM capacitors have to undergo annealing in a forming gas atmosphere at 400 °C after metallization at the back end of line (BEOL) stage, to reduce interfacial traps in cell transistors and to lessen row hammering effects from the interconnect metal layer. It is reported that the hydrogen reduction of RuO_2 and $SrRuO_3$ layers inevitably occurs even at relatively low temperatures of <400 °C.[12-13] The reduction results in severe degradation in the structural and electrical properties of the capacitors. RuO_2 has a small formation energy of -45.2 kcal·mol^{-1} at 400 °C [14] and the hydrogen reduction reaction has a negative Gibbs free energy of -41.9 kcal·mol^{-1} at 400 °C as well.[12] This indicates that such reduction problems stem from the characteristics of the materials themselves, and are hardly improved by process control alone.

In this study, MoO_2 is proposed as an alternative oxide electrode for DRAM capacitors. MoO_2 is a metallic conductor. The work function of MoO_2 is reported to be larger than 6 eV.[15-17] It crystallizes in a monoclinic cell and has a distorted rutile

[a] Department of Materials Science and Engineering, Northwestern University, Evanston, IL 60208, United States
[b] Center for Electronic Materials, Korea Institute of Science and Technology, Seoul, 02792, South Korea. *E-mail: s.k.kim@kist.re.kr
[c] Department of Materials Science and Engineering, and Inter-University Semiconductor Research Center, Seoul National University, Seoul, 08826, South Korea
†These two authors equally contributed to this work.

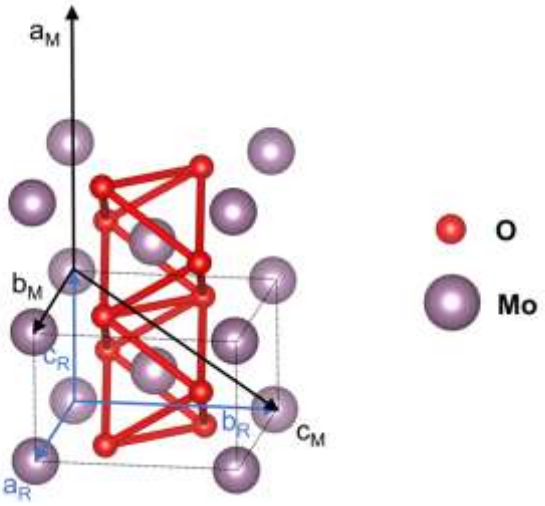

Fig. 1 Crystal structure of monoclinic (M) MoO_2. The unit cell of the distorted rutile (R) structure is shown with dashed lines.

structure as shown in Fig. 1. The lattice constants of the distorted rutile MoO_2 are 0.486 and 0.282 nm for the a- and c-axis, respectively. The lattice mismatches between rutile TiO_2 and MoO_2, defined as $(d_{TiO2} - d_{MoO2})/d_{MoO2}$, are calculated to be only -5.49 % for the *a*-axis and 4.70 % for the *c*-axis, respectively. Therefore, MoO_2 was reported to induce the formation of a high-k material, rutile TiO_2, on its surface by conventional growth techniques at relatively low temperatures.[18] The previous report[18], however, did not take into account the thermal stability in oxidation or reduction ambient for TiO_2/MoO_2 stack which is crucial for the fabrication of DRAMs.

Although the hydrogen reduction of MoO_2 has been reported elsewhere, the reduction reaction occurs only above 600 °C.[19, 20] Hence, it is expected that thermal treatment after metallization in BEOL would not reduce MoO_2. One concern is the possibility of transformation of MoO_2 into MoO_3 because this form is more stable than MoO_2. Thus, in this work, capacitors composed of TiO_2/MoO_2 stacks were fabricated to verify the possibility of MoO_2 as a capacitor electrode. The stability of the structural and electrical properties of MoO_2 was investigated after annealing in both a forming gas and an O_2 atmosphere.

Experimental

MoO_2 thin films were grown on quartz glass substrates by pulsed laser deposition (PLD) using a KrF excimer laser (λ = 248 nm). The excimer laser was focused on a hot-pressed MoO_3 target with a fluence of 7.3 J·cm^{-2} at a repetition rate of 2 Hz. The growth of MoO_2 films was performed at 600 °C under an oxygen partial pressure of 1 mTorr, and a background pressure of <5 × 10^{-7} Torr. The distance between the target and the substrate was fixed at 10 cm. Under these conditions, each laser pulse delivers a sub-monolayer of the desired film, implying very high precision. Subsequently, TiO_2 films were grown on the MoO_2 by atomic layer deposition (ALD) with titanium tetrakis-isopropoxide and O_3 at 250 °C. The O_3

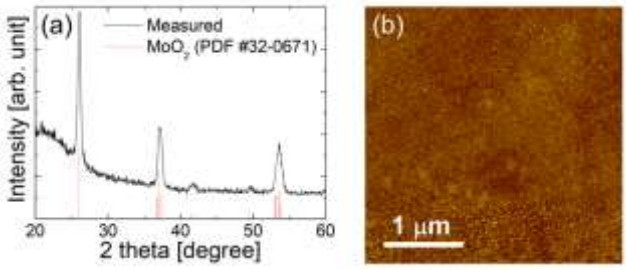

Fig. 2 (a) GIXRD pattern and (b) AFM image of the PLD-grown 80 nm-thick MoO_2 film on quartz glass substrate.

feeding time was fixed at 5 s. Detailed information of the growth conditions is given in the literature.[21] To investigate the thermal stability of the TiO_2/MoO_2 stack structure, the TiO_2/MoO_2 stacks were annealed at 400 °C in a forming gas (H_2(4%)/Ar) or O_2 atmosphere for 30 min.

To identify the crystal structure of the films, grazing-incident X-ray diffraction (GIXRD) was used with incident angle of 1°. The surface morphology was examined by atomic force microscopy (AFM). An Auger electron spectroscopy (AES) analysis was attempted to examine the chemical composition in the direction of the film thickness. The crystal structure coherency of the TiO_2/MoO_2 was observed using cross-sectional high-resolution transmission electron microscopy (HRTEM).

Pt top electrodes were formed on the TiO_2/MoO_2 stacks by DC sputtering using a shadow mask. The insulating and dielectric properties of the capacitors composed of Pt/TiO_2/MoO_2 were obtained using an Agilent 4155A semiconductor parameter analyzer and an Agilent 4294A precision impedance analyzer.

Results and Discussion

It is essential to obtain single-phase, well-crystallized MoO_2 films to examine the possibility of MoO_2, the material itself, as an electrode for memory capacitors. Here, using the exquisite control of the deposition conditions provided by PLD, high-quality MoO_2 films, which could serve as a material platform, were successfully synthesized. Figure 2 (a) shows the GIXRD pattern of the 80 nm-thick MoO_2 film grown on quartz glass substrate. All the observed peaks correspond to Bragg peaks of monoclinic MoO_2. Three intense Bragg peaks corresponding to MoO_3 are located at 22.2, 22.8, and 23.9° for the (002), (020), and (20-2) planes, respectively. These peaks are not observed in Fig. 2 (a). This might be attributed to the growth conditions such as the low oxygen pressure and high temperature. The resistivity of the grown MoO_2 films measured by the van der Pauw method is 1.5 × 10^{-4} ohm·cm. This low resistivity qualifies the films to act as an electrode in DRAM devices. Indeed, MoO_2 is known as a metallic conductor, with a reported resistivity of 1.6 × 10^{-4} ohm·cm for MoO_2 grown by chemical vapor deposition.[22] Considering MoO_3 has a low intrinsic conductivity, these results support the conclusion that the grown films are well crystallized into a single-phase MoO_2 without inclusion of MoO_3. Moreover, since no carbon impurity was included in the MoO_2 grown by PLD, the MoO_2

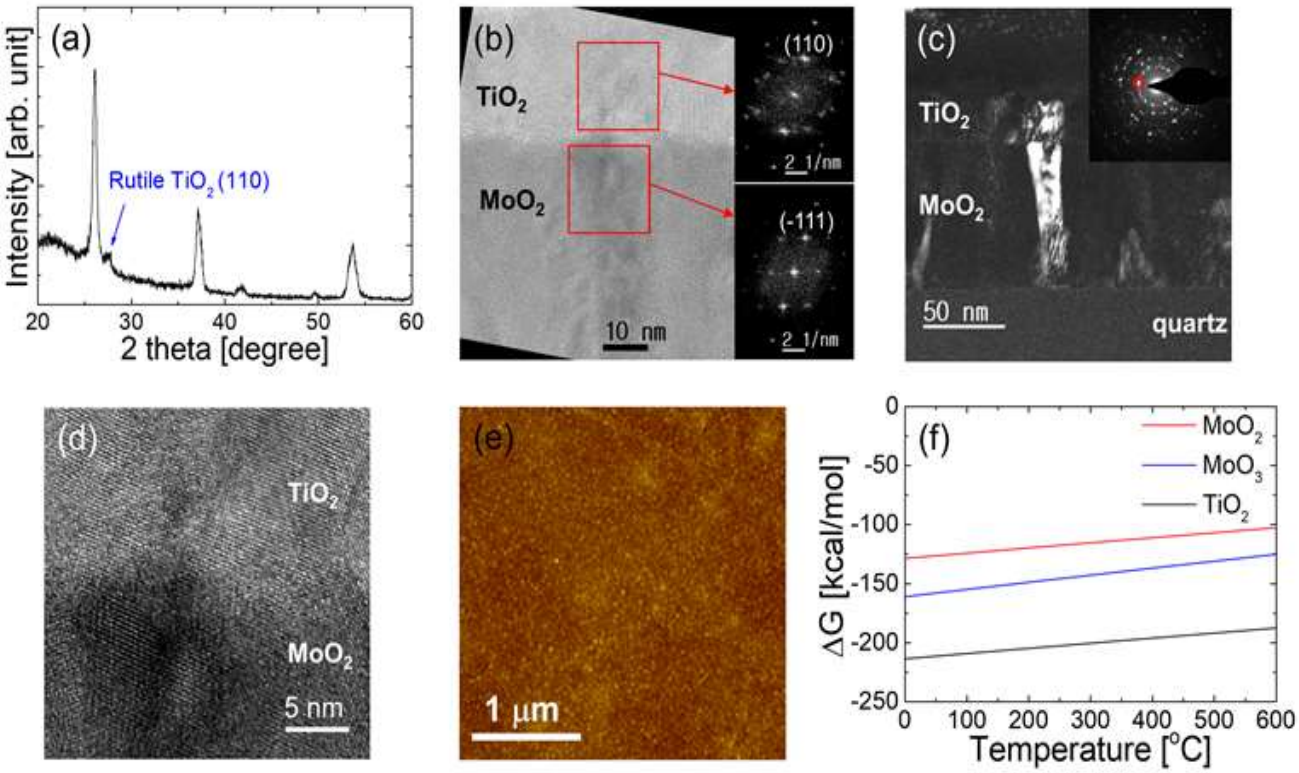

Fig. 3 (a) GIXRD pattern of the ALD-grown TiO_2 film on MoO_2. (b) high-resolution, (c) dark-field, and (d) magnified high-resolution TEM images of as-grown 25 nm-thick TiO_2 film on MoO_2. (e) AFM image of as-grown 15 nm-thick TiO_2 film on MoO_2. (f) Gibbs free energies of MoO_2, MoO_3, and TiO_2 as a function of temperature.[14]

was grown with minimal of contamination compared with the films grown by the conventional metal organic chemical vapor deposition or ALD. Figure 2 (b) shows the AFM image of the 80 nm-thick MoO_2 film. The root-mean-squared (RMS) roughness of the AFM image is as low as 1.1 nm. The surface morphology is smooth enough to exclude adverse effects caused by surface roughening where MoO_2 is used as the bottom electrode for the capacitors. Therefore, the grown MoO_2 films are appropriate for use in the investigation of the viability of such capacitor electrodes with a TiO_2 layer.

There are two different TiO_2 crystal structures of anatase and rutile. Conventional growth techniques including ALD usually form a TiO_2 film of an anatase structure, which has a relatively low k value of ~40. A very high temperature of ~1000 °C is required to transform the anatase into rutile TiO_2, a high temperature phase with a much higher k value.[23] Without the aid of the post-deposition annealing, the rutile TiO_2 is only formed on lattice-matched substrates such as RuO_2 and IrO_2.[24-25] Rutile TiO_2 was also expected to be formed on the MoO_2 electrode because of the structural similarity between rutile TiO_2 and MoO_2. Figure 3 (a) shows the GIXRD pattern of 25 nm-thick TiO_2 grown on MoO_2 by ALD at 250 °C. The GIXRD pattern displays a rutile TiO_2 (110) peak at 27.5 ° as well as MoO_2 peaks. No peak corresponding to anatase TiO_2 is observed. To further identify the reason why rutile TiO_2 is formed on MoO_2, the microstructure of the TiO_2/MoO_2 stack structure was examined by TEM. Figure 3 (b) shows the HRTEM image of 25 nm-thick TiO_2 grown on MoO_2. The insets in Fig. 3 (b) indicate the fast Fourier transform patterns from the red boxes located in MoO_2 and TiO_2 in Fig. 3 (b). The reciprocal lattice points corresponding to (-111) plane of monoclinic MoO_2 and (110) plane of rutile TiO_2 are collinear with comparable d-spacings (0.342 nm for MoO_2 (-111) plane and 0.325 nm for rutile TiO_2 (110) plane), which indicates the same orientation relationship between TiO_2 film and MoO_2 substrate. Figure 3 (c) shows the dark-field TEM image of the 25 nm-thick TiO_2 grown on MoO_2 obtained from the diffraction spot indicated in the inset. It was found from the dark-field TEM image that the grain in the MoO_2 layer has the same crystallographic orientation as the TiO_2 grain on it. This orientation relationship is observed in the whole TiO_2/MoO_2 stack. These support the supposition that the rutile TiO_2 layer is inductively formed on MoO_2 through the reduction in the interfacial energy caused by the epitaxial relationship between rutile TiO_2 and monoclinic MoO_2.

The MoO_2 surface could be partially transformed into MoO_3 during the initial growth stage of TiO_2 because MoO_2 is exposed to O_3 with a strong oxidation potential. Indeed, the Gibbs free energy for the reaction of $3MoO_2 + O_3 \rightarrow 3MoO_3$ has a negative value of -126 kcal·mol^{-1} at 250 °C, which is the TiO_2 growth temperature. MoO_3 impedes the formation of rutile TiO_2. Therefore, the presence of MoO_3 at the interface between TiO_2 and MoO_2 is examined. Here, the feeding time of O_3 is fixed to 5 s for the growth of the TiO_2 film. In Fig. 3 (d), the HRTEM image of the 25 nm-thick TiO_2 grown on MoO_2, the excellent alignment of the rutile TiO_2 and MoO_2 lattices can be seen. The MoO_3 phase is not observed at the interface despite the spontaneity of the oxidation reaction of MoO_2 with O_3.

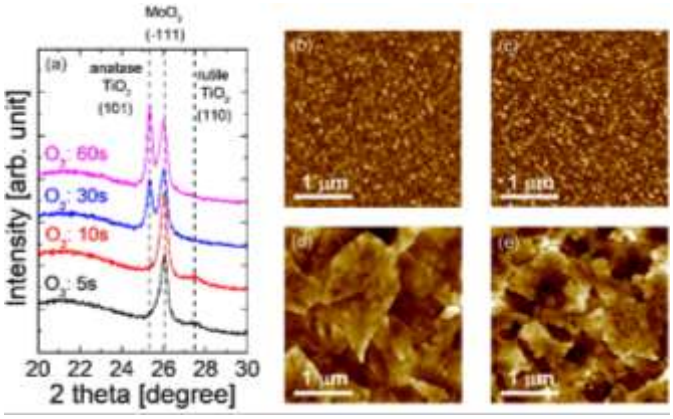

Fig. 4 (a) GIXRD patterns of 25 nm-thick TiO_2 films grown on MoO_2 by ALD with various O_3 feeding times of 5, 10, 30, and 60 s. AFM images of 25 nm-thick TiO_2 films grown on MoO_2 by ALD with various O_3 feeding times of (b) 5, (c) 10, (d) 30, and (e) 60 s, respectively.

Figure 3 (e) shows an AFM image of the 15 nm-thick TiO_2 film grown on MoO_2. The RMS roughness is as low as 1.1 nm, comparable to the value of the MoO_2 film surface (Fig. 2 (b)). Further oxidation of the MoO_2 surface by exposure to O_3 would result in the surface roughening, and thus, a smooth surface also verifies the absence of MoO_3 at the interface between TiO_2 and MoO_2. This is likely because most of the O_3 injected during ALD of TiO_2 is consumed in reaction with the adsorbed Ti precursors rather than in oxidizing MoO_2 into MoO_3. The formation energies of TiO_2 are much lower than those of MoO_2 and MoO_3 as shown in Fig. 3 (f).[14] Such low formation energies of TiO_2 support the absence of MoO_3 at the TiO_2/MoO_2 interface.

However, the supply of excess O_3 beyond the amounts required for the reaction with the Ti precursors may result in the transformation of MoO_2 into MoO_3, consequently leading to the formation of anatase TiO_2 with a low k value on it. To verify the influence of the O_3 flux, the feeding time of O_3 for the growth of TiO_2 films is varied from 5 s to 60 s. Figure 4 (a) shows the GIXRD patterns of 25 nm-thick TiO_2 films grown on MoO_2 with various O_3 feeding times of 5, 10, 30, and 60 s, respectively. A rutile TiO_2 (110) peak is observed up to an O_3 feeding time of 10 s while above an O_3 feeding time of 30 s, the rutile TiO_2 peak disappears and an anatase TiO_2 (101) peak is observed. The surface morphology of the films is also examined to further understand the phase change of TiO_2 films. Figures 4 (b)-(e) show the AFM images of 25 nm-thick TiO_2 films grown on MoO_2 with various O_3 feeding times of 5, 10, 30, and 60 s, respectively. TiO_2 films grown with O_3 feeding times of 5 and 10 s, which are crystallized into rutile, show relatively small grains whereas TiO_2 films grown with long O_3 feeding times of 30 and 60 s display very large grains, which are much larger than the MoO_2 grains. This large TiO_2 grains are the unique

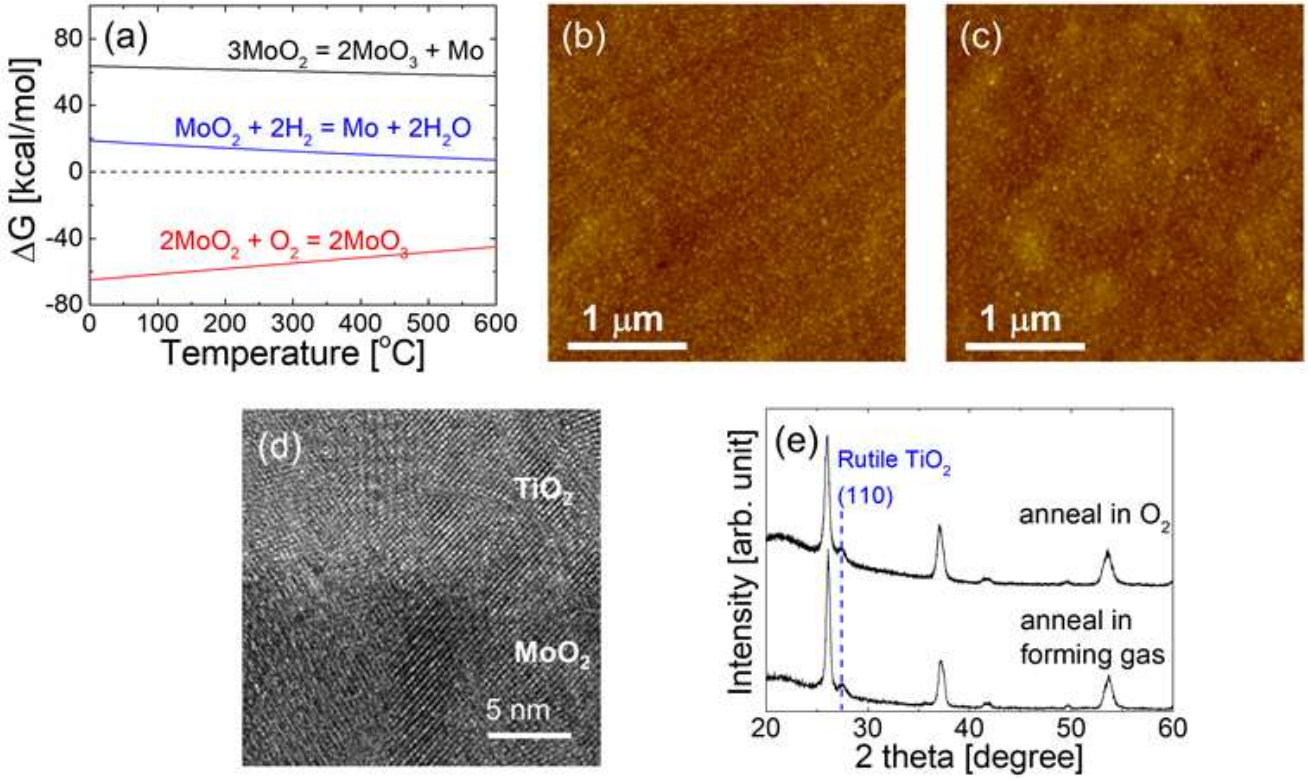

Fig. 5 (a) Gibbs free energies for the plausible reactions of MoO_2 such as disproportionation, and reactions of MoO_2 with H_2 and O_2, as a function of temperature.[14] AFM images of 15 nm-thick TiO_2/MoO_2 annealed in (b) forming gas and (c) O_2 atmospheres. (d) HRTEM image of 25 nm-thick TiO_2/MoO_2 annealed in a forming gas atmosphere. (e) GIXRD patterns of 25 nm-thick TiO_2/MoO_2 annealed in forming gas and O_2 atmospheres.

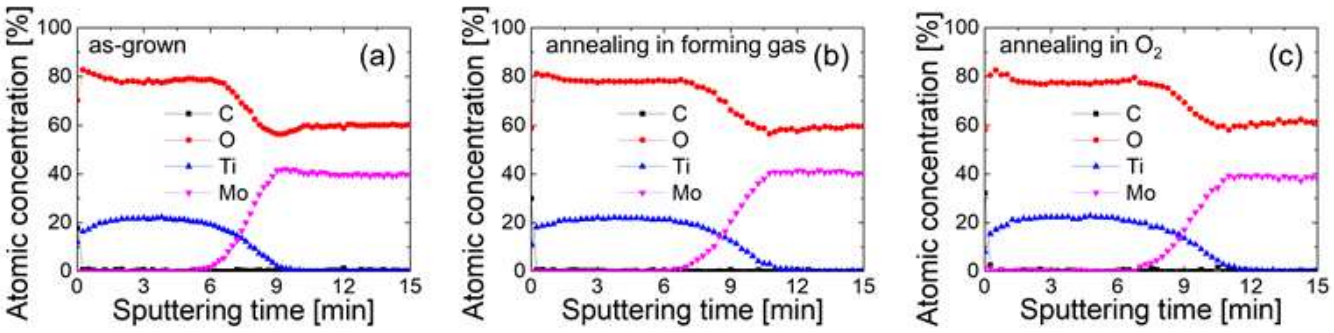

Fig. 6 AES depth profiles of (a) the as-grown 25 nm-thick TiO_2/MoO_2 and the stacks annealed under (b) forming gas and (c) O_2 atmosphere, respectively.

characteristic of the anatase-structured TiO_2 films grown by ALD.[21] Therefore, optimization of the O_3 flux is the key to suppressing the formation of MoO_3.

The thermal stability of the TiO_2/MoO_2 stacks was investigated. Theoretical calculations for plausible reactions are used to understand the thermal stability of the TiO_2/MoO_2 stacks. The disproportionation reaction of MoO_2 is shown below:

$3MoO_2 \rightarrow 2MoO_3 + Mo$ (1)

The Gibbs free energies of the reaction are positive in the temperature range of 0 to 600 °C (Fig. 5 (a)).[14] This indicates that MoO_2 is not spontaneously decomposed in this temperature range. The plausible reactions of MoO_2 with H_2 and O_2 are shown below:

$MoO_2 + 2H_2 \rightarrow Mo + 2H_2O$ (2)

$2MoO_2 + O_2 \rightarrow 2MoO_3$ (3)

Reaction (2), above, has positive Gibbs free energies in the temperature range of 0 to 600 °C as shown in Fig. 5 (a).[14] Therefore, MoO_2 was not expected to spontaneously reduce in a forming gas atmosphere. Conversely, reaction (3) has negative Gibbs free energies in the same temperature range (Fig. 5 (a)), suggesting that MoO_2 would be unstable in an O_2 atmosphere. To verify this thermal stability expectation, the structural properties of the TiO_2/MoO_2 stacks are examined after annealing at 400 °C in a forming gas and an O_2 atmosphere. Figures 5 (b) and (c) show AFM images of the 15 nm-thick TiO_2 films on MoO_2 annealed at 400 °C in (b) a forming gas and (c) and O_2 atmosphere for 30 minutes, respectively. Both film surfaces are smooth with a 1 nm RMS roughness, consistent with that of the as-grown film in Fig. 3 (e). No distinct change in the surface morphology is observed after annealing in the forming gas and O_2 atmospheres. The authors previously reported that after annealing in a forming gas, the RuO_2 surface was seriously damaged due to the formation of cleavages and pinholes.[12] This result indicates that the TiO_2/MoO_2 stacks are thermally stable under both forming gas and O_2 atmospheres.

The reduction resistance of the oxide electrode in an H_2 atmosphere is particularly critical because the annealing process in a forming gas atmosphere after metallization in BEOL is indispensable. Hence, the structural stability of the TiO_2/MoO_2 stack in forming gas deserves further study. Figure 5 (d) shows the HRTEM image of the 25 nm-thick TiO_2/MoO_2 structure annealed at 400 °C in a forming gas atmosphere. The HRTEM image shows a sharp interface between TiO_2 and MoO_2. No trace of the reduction of MoO_2 is observed. Thus, the crystallinity of the TiO_2 layer was not disturbed by the annealing in a forming gas atmosphere. The excellent alignment of the TiO_2 and MoO_2 lattices was preserved even after annealing in the reduction atmosphere.

Figure 5 (e) shows GIXRD patterns of the 25 nm-thick TiO_2 films on MoO_2 after annealing at 400 °C in forming gas and O_2 atmospheres. The XRD patterns are consistent with the XRD pattern of as-grown TiO_2/MoO_2 in Fig. 3 (a). Both XRD patterns show a rutile TiO_2 (110) peak as well as MoO_2 peaks irrespective of the ambient atmosphere. No peak corresponding to the reduced or oxidized phases of MoO_2 is detected even after the ambient annealing.

To further elucidate the thermal stability of the TiO_2/MoO_2 stack structure, the chemical composition was examined along the film thickness. Figures 6 (a)-(c) show the AES depth profiles of (a) the as-grown 25 nm-thick TiO_2/MoO_2 and the stacks annealed under (b) a forming gas and (c) an O_2 atmosphere, respectively. No distinct change in the depth profiles was observed after annealing in the two atmospheres. In particular, the ambient annealing did not change the O/Mo ratio in the stacks, demonstrating the viability of MoO_2 as the electrode for DRAM capacitors. A slight change in the composition gradient was observed at the interface after the post-annealing. However, the sputtering time required to reach the TiO_2/MoO_2 interface also increased after the post-annealing. This indicates the densification of the TiO_2 films by the post-annealing at 400 °C. Hence, the change in the composition gradient seems to be due to the densification of the TiO_2 films by the post-annealing. It should be noted that

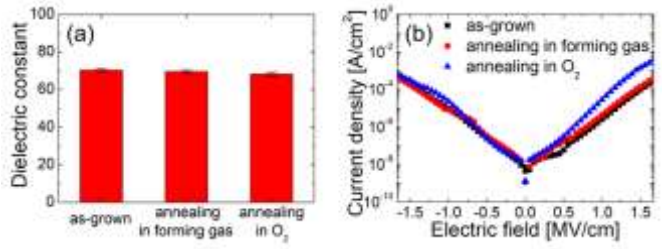

Fig. 7 (a) Dielectric constant and (b) leakage current density *vs.* applied electric field curves of the Pt/18-nm-thick TiO_2/MoO_2 capacitors. Three different samples: the as-grown TiO_2 film, and the two TiO_2 films annealed in forming gas and O_2 atmospheres, respectively, are used to compare the electrical properties.

the atomic concentrations in AES must be considered only as relative numbers because there was no appropriate standard for AES calibration.

Although the excellent thermal stability of MoO_2 in a forming gas atmosphere could be understood from the thermodynamic calculation, the experimental results on the TiO_2/MoO_2 annealed in an O_2 atmosphere seem to contradict the theoretical expectation. This may be attributed to the kinetic limit of the MoO_2 oxidation reaction at the annealing temperature. In addition, the existence of TiO_2 on the MoO_2 is likely to suppress the oxidation of the lower MoO_2 layer.

The electrical properties of capacitors composed of Pt/18-nm-thick TiO_2/MoO_2 depending on the annealing atmosphere were examined. Figure 7 (a) shows the k value of the as-grown TiO_2 film and the TiO_2 films annealed in forming gas and O_2 atmospheres. All TiO_2 films have a high k of approximately 70, and degradation in the dielectric constant by annealing in the ambient atmospheres was not observed. Anatase TiO_2, which is generally formed by ALD, has a relatively low k of 40. This supports the formation of rutile TiO_2 on the MoO_2, which is consistent with the results for the crystal structure in Figs. 3 and 5. Figure 7 (b) shows the leakage current density *vs.* electric field curves of the Pt/18 nm-thick TiO_2/MoO_2 capacitors. No significant degradation was observed in the leakage currents even after annealing in both forming gas and O_2 atmospheres. Although a slight increase in the leakage currents of the capacitor was observed after annealing in an O_2 atmosphere, the change in the leakage currents may not be attributed to the formation of MoO_3. The dielectric constant of the TiO_2 was not changed by annealing in an O_2 atmosphere, as shown in Fig. 7 (a). The formation of MoO_3 would result in a decrease in the dielectric constant because MoO_3 is an insulator. It was reported that the leakage currents of the TiO_2/RuO_2 capacitor increased substantially (by a factor of more than 10^4) after annealing in a forming gas atmosphere, because of the reduction of the RuO_2 bottom electrode. These results indicate that the electrical, structural, and chemical properties of the TiO_2/MoO_2 stacks have excellent thermal stability.

Conclusions

MoO_2 was proposed as a thermally stable oxide electrode for DRAM capacitors. The MoO_2 films showed a very low resistivity of 1.5×10^{-4} ohm·cm, which is sufficiently low for them to be used as electrodes in DRAM capacitors. The MoO_2 film induced the formation of rutile TiO_2, a promising high-k dielectric, on its surface due to the structural coherency between rutile TiO_2 and MoO_2. In addition, the TiO_2/MoO_2 stacks showed excellent thermal stability of the structural and electrical properties after annealing at 400 °C in both forming gas and O_2 atmospheres. As capacitors in DRAM inevitably suffer from thermal stress in ambient atmospheric conditions, these findings demonstrate that MoO_2 is a promising electrode material for use in DRAM capacitors. For further study, it would be necessary to develop an ALD process for preparing MoO_2 films with smaller thickness (< 10 nm) and high conformality in high aspect ratio structures for practical applications in DRAMs.

Conflicts of interest

There are no conflicts to declare.

Acknowledgements

This work was supported by the National Research Foundation of Korea Grant funded by the Korean government (NRF-2018R1A2B2007525) and the Korea Institute of Science and Technology (KIST through 2E28210). Work performed at Northwestern University was funded under NSF-DMREF 1729016. This work made use of the MatCI Facility which receives support from the MRSEC Program (NSF DMR-1720139) of the Materials Research Center at Northwestern University.

References

(1) Kim, S. K.; Popovici, M. Future of dynamic random-access memory as main memory. *MRS Bull.* **2018,** *43* (5), 334-339.

(2) Kim, S. K.; Kim, W. D.; Kim, K. M.; Hwang, C. S.; Jeong, J. High dielectric constant TiO_2 thin films on a Ru electrode grown at 250 degrees C by atomic-layer deposition. *Appl. Phys. Lett.* **2004,** *85* (18), 4112-4114.

(3) Kim, S. K.; Lee, S. W.; Han, J. H.; Lee, B.; Han, S.; Hwang, C. S. Capacitors with an Equivalent Oxide Thickness of < 0.5 nm for Nanoscale Electronic Semiconductor Memory. *Adv. Funct. Mater.* **2010,** *20* (18), 2989-3003.

(4) Kim, S. K.; Choi, G. J.; Lee, S. Y.; Seo, M.; Lee, S. W.; Han, J. H.; Ahn, H. S.; Han, S.; Hwang, C. S. Al-doped TiO_2 films with ultralow leakage currents for next generation DRAM capacitors. *Adv. Mater.* **2008,** *20* (8), 1429-1435.

(5) Kim, S. K.; Kim, K. M.; Jeong, D. S.; Jeon, W.; Yoon, K. J.; Hwang, C. S. Titanium dioxide thin films for next-generation memory devices. *J. Mater. Res.* **2013,** *28* (3), 313-325.

(6) Lee, W.; Han, J. H.; Jeon, W.; Yoo, Y. W.; Lee, S. W.; Kim, S. K.; Ko, C. H.; Lansalot-Matras, C.; Hwang, C. S. Atomic Layer Deposition of $SrTiO_3$ Films with Cyclopentadienyl-Based Precursors for Metal-Insulator-Metal Capacitors. *Chem. Mater.* **2013,** *25* (6), 953-961.

(7) Lima, L. P. B.; Diniz, J. A.; Doi, I.; Godoy Fo, J. Titanium nitride as electrode for MOS technology and Schottky diode: Alternative extraction method of titanium nitride work function. *Microelectron. Eng.* **2012,** *92*, 86-90.

(8) Han, J. H.; Han, S.; Lee, W.; Lee, S. W.; Kim, S. K.; Gatineau, J.; Dussarrat, C.; Hwang, C. S. Improvement in the leakage current characteristic of metal-insulator-metal capacitor by adopting RuO_2 film as bottom electrode. *Appl. Phys. Lett.* **2011,** *99* (2), 022901.

(9) Popescu, D.; Popescu, B.; Jegert, G.; Schmelzer, S.; Boettger, U.; Lugli, P. Feasibility Study of $SrRuO_3/SrTiO_3/SrRuO_3$ Thin Film Capacitors in DRAM Applications. *IEEE T. Electron Dev.* **2014,** *61*, 2130-2135.

(10) Murakami, K.; Rommel, M.; Hudec, B.; Rosová, A.; Hušeková, K.; Dobročka, E.; Rammula, R.; Kasikov, A.; Han, J. H.; Lee, W.; Song, S. J.; Paskaleva, A.; Bauer, A. J.; Frey, L.; Fröhlich, K.; Aarik, J.; Hwang, C. S. Nanoscale Characterization of TiO_2 Films Grown by Atomic Layer

Deposition on RuO_2 Electrodes. *ACS Appl. Mater. Interface* **2014,** *6* (4), 2486-2492.
(11) Ahn, J.-H.; Kim, J.-Y.; Kim, J.-H.; Roh, J.-S.; Kang, S.-W. Enhanced Dielectric Properties of $SrTiO_3$ Films with a $SrRuO_3$ Seed by Plasma-Enhanced Atomic Layer Deposition. *Electrochem. Solid-State Lett.* **2009,** *12* (2), G5-G8.
(12) Cho, C. J.; Noh, M.-S.; Lee, W. C.; An, C. H.; Kang, C.-Y.; Hwang, C. S.; Kim, S. K. Ta-Doped SnO_2 as a reduction-resistant oxide electrode for DRAM capacitors. *J. Mater. Chem. C* **2017,** *5* (36), 9405-9411.
(13) Mlynarczyk, M.; Szot, K.; Petraru, A.; Poppe, U.; Breuer, U.; Waser, R. Surface layer of $SrRuO_3$ epitaxial thin films under oxidizing and reducing conditions. *J. Appl. Phys.* **2007,** *101* (2), 023701.
(14) *HSC Chemistry 5.11*, 2002.
(15) Liang, Y.; Tracy, C.; Weisbrod, E.; Fejes, P.; Theodore, N. D. Effect of SiO_2 incorporation on stability and work function of conducting MoO_2. *Appl. Phys. Lett.* **2006,** *88* (8), 081901.
(16) Wu, C.-I.; Lin, C.-T.; Lee, G.-R.; Cho, T.-Y.; Wu, C.-C.; Pi, T.-W. Electronic and chemical properties of molybdenum oxide doped hole injection layers in organic light emitting diodes. *J. Appl. Phys.* **2009,** *105* (3), 033717.
(17) Lee, W.-J.; Parmar, N. S.; Choi, J.-W. High work function MoO2 and ReO_2 contacts for p-type Si and GaN by a room-temperature non-vacuum process. *Mat Sci Semicon Proc* **2017,** *71*, 374-377.
(18) Xiangxin Rui, P. K., Hanhong Chen, Sandra Malhotra Enhanced work function layer supporting growth of rutile phase titanium oxide. US8415657B2, 2013.
(19) Dang, J.; Zhang, G.-H.; Chou, K.-C. Study on kinetics of hydrogen reduction of MoO_2. *Int. J. Refract. Met. Hard Mater.* **2013,** *41*, 356-362.
(20) Orehotsky, J.; Kaczenski, M. The kinetics of the hydrogen reduction of MoO_2 powder. *Mater. Sci. Eng.* **1979,** *40* (2), 245-250.
(21) Cho, C. J.; Kang, J.-Y.; Lee, W. C.; Baek, S.-H.; Kim, J.-S.; Hwang, C. S.; Kim, S. K. Interface Engineering for Extremely Large Grains in Explosively Crystallized TiO_2 Films Grown by Low-Temperature Atomic Layer Deposition. *Chem. Mater.* **2017,** *29* (5), 2046-2054.
(22) Xie, Q.; Zheng, X.; Wu, D.; Chen, X.; Shi, J.; Han, X.; Zhang, X.; Peng, G.; Gao, Y.; Huang, H. High electrical conductivity of individual epitaxially grown MoO_2 nanorods. *Appl. Phys. Lett.* **2017,** *111* (9), 093505.
(23) Jin, C.; Liu, B.; Lei, Z.; Sun, J. Structure and photoluminescence of the TiO_2 films grown by atomic layer deposition using tetrakis-dimethylamino titanium and ozone. *Nanoscale Res. Lett.* **2015,** *10* (1), 95.
(24) Fröhlich, K.; Aarik, J.; Ťapajna, M.; Rosová, A.; Aidla, A.; Dobročka, E.; Hušková, K. Epitaxial growth of high-κ TiO_2 rutile films on RuO_2 electrodes. *J. Vac. Sci. Technol. B* **2009,** *27* (1), 266-270.
(25) Kim, S. K.; Han, S.; Han, J. H.; Lee, W.; Hwang, C. S. Atomic layer deposition of TiO_2 and Al-doped TiO_2 films on Ir substrates for ultralow leakage currents. *Phys Status Solidi-R* **2011,** *5* (8), 262-264.

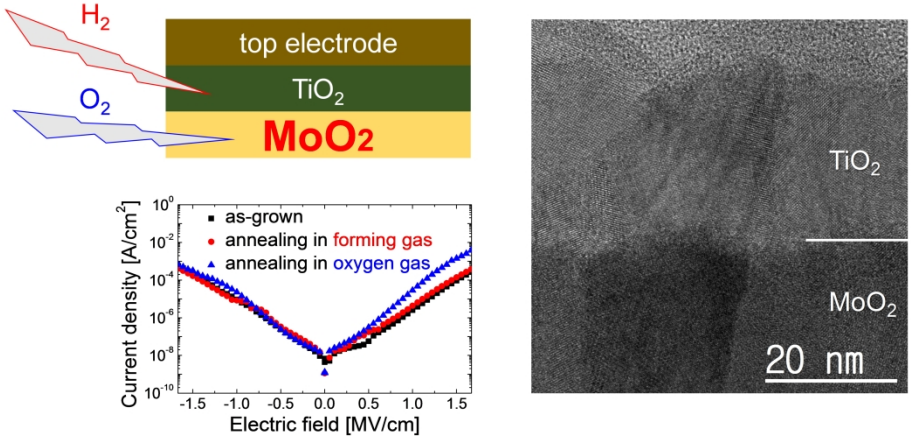

MoO_2 is a promising oxide electrode with an excellent thermal stability for the next-generation DRAM capacitor.

TOC